



Numerical Modelling of Flow over Single-Step Broad-Crested Weir Using FLOW-3D and HEC-RAS

Shaker Abdulatif Jalil and Jihan Mahmood Qasim

Water Resources Engineering Department, College of Engineering, University of Duhok, Iraq
shakerjalil@yahoo.com and Jihan.mahmood@uod.ac

ABSTRACT

In this study, the free flow over the single-step weir was simulated using the ($k-\epsilon$ model) of FLOW-3D and the (Steady-Flow model) of HEC-RAS. The predicted results were assessed by laboratory observations involving different flow situations. The numerical models demonstrated ability to capture the flow pattern upstream the weir with inaccuracy of 0.52% and 0.59%, respectively. However, the gradually varied flow over the crest was better computed by FLOW-3D with inaccuracy of 1.57% against 2.48% in HEC-RAS. In addition, HEC-RAS predicted higher brink depths, especially at higher flow rates. The models predicted the critical depth and its relation to brink depth with satisfactory accuracy. Furthermore, the (y_c/y_b) ratio was 1.5687 in FLOW-3D versus 1.0193 in HEC-RAS. In the simulation of the nape flow falling from the weir crest and step, HEC-RAS showed limited ability to produce these curved profiles past vertical faces, as compared to FLOW-3D. On the other hand, both models did not simulate efficiently the supercritical flow before the hydraulic jump but well estimated the jump location.

KEYWORDS: Single-step weir, FLOW-3D, HEC-RAS, numerical modelling, water surface profile, hydraulic jump, critical depth, brink depth, nape flow

INTRODUCTION

The great development in Computational Fluid Dynamics motivates the simulation of different types of hydraulic structures in order to examine their performance under different flow situations. The HEC-RAS and FLOW-3D software are two common numerical models that are continuously evaluated to see their abilities and limitations. Gonzalez (1999) and Cook (2008) compared HEC-RAS and FESWMS (Finite Element Surface Water Modelling System) in simulating floodplain. It was found that HEC-RAS was easy and quick while FESWMS produced more accurate results. Siddique-E-Akbore *et al.* (2011) compared HEC-RAS with Envisat (satellite altimetry mission model) in estimating water levels in a river of deltaic environments. The highest level of agreement between the models was observed for high flows. Toombes and Chanson (2011) examined HEC-RAS, FLOW-3D, MIKE 11 and MIKE 21 to model rapidly and gradually varied flow. It was observed that FLOW-3D achieved excellent agreement to the physical model data and that HEC-RAS could model supercritical and subcritical flow and predict the location of a hydraulic jump with reasonable accuracy. Rady (2011) used FLOW-3D to estimate a relationship for the discharge coefficient of rectangular sharp-crested weirs. It was noted that the model demonstrated advantages for examining velocity vectors and pressure pattern over the weirs. Mohammed and Qasim (2012) compared HEC-RAS with AdH (Adaptive Hydraulics model) to simulate the free flow over trapezoidal-profile weirs. It was noticed that HEC-RAS could capture the overall

features of the flow profile with good accuracy in a short computational time. Crookston, Paxson and Savage (2012) utilized FLOW-3D to obtain the head-discharge relationship for the labyrinth weir. The predicted results were found in agreement with physical modelling. Hoseini (2014) used FLOW-3D to simulate the free surface flow over the triangular broad-crested weir. The simulation results were found in reasonable agreement with experimental observations. Akbar, Habib and Hassan (2015) analysed the current properties in channel junction based on the hydraulic jump due to junction. The hydraulic jump was simulated using FLUENT and FLOW-3D software. It was concluded that the FLOW-3D results were far more accurate and closer to the experimental results.

In the present study, the flow phenomenon over the single-step weir is investigated using numerical modelling and laboratory measurements. The flow pattern before, over and after the weir involves uniform, gradually and rapidly varied flows occurring along a relatively short distance. It includes nappe flows and hydraulic jumps. The $k-\epsilon$ turbulence model of FLOW-3D and the Steady-Flow module of HEC-RAS are compared in different aspects in simulating these types of flow.

GOVERNING EQUATIONS OF FLOW-3D

The physical laws of conservation are the core of controlling the behavior of materials in motion or in state; these conservation laws are mass, momentum and energy. All fluid properties are functions of space and time (Graebel, 2007).

The mass conservation law states that the rate of increase of mass in a control volume should equal the net rate of mass flow into the volume from its surface. The statement is mathematically represented in differential form:

$$\frac{\partial \rho}{\partial t} + \text{div}(\rho \mathbf{U}) = 0 \quad \dots (1)$$

where \mathbf{U} is the velocity vector in the three directions (m/sec), and ρ is the mass density (kg/m³).

Most types of flow in engineering practice become unstable when Reynolds number, Re , increases to reach a certain value. In this unstable state the ratio of inertia forces relative to viscous forces become high generating turbulent flow having chaotic and random fluctuation of the velocity components with the time. This complicated structure of flow has been simplified by Reynolds decomposition with the help of fundamental of micro-scale theory of Kolmogorov cited in Versteeg and Malalasekera (2007). Fluctuation properties of turbulent flow can be presented by time average rules. As the main fluctuating flow parameters are the velocity \mathbf{U} and pressure P , the Reynolds decomposition of the sum of means given in Equation (2) can be implanted in the instantaneous continuity equation and in Navier–Stokes equations of incompressible flow:

$$u = U + u', v = V + v', w = W + w', p = P + p' \quad \dots (2)$$

where u, v, w are the velocity components along the x, y, z axes, respectively (m/sec). The replacement of the sums in the conservative equations of mass and momentum leads to the continuity equation for the mean flow equation (3) and the time-average momentum equation (4) in the x -direction as stated by Versteeg and Malalasekera (2007). The equations in the y - and z -directions can be written in a similar manner:

$$\text{div } \mathbf{u} = \text{div } \mathbf{U} = 0 \quad \dots (3)$$

$$\frac{\partial U}{\partial t} + \text{div}(UU) + \text{div}(\overline{u'u'}) = -\frac{1}{\rho} \frac{\partial P}{\partial y} + \nu \text{div}(\text{grad}(U)) \quad \dots (4)$$



The terms $div(\overline{u'u'})$ are related to the convection of momentum transfer due to eddy formation. Equation (4) can be rewritten to show that the terms $(div(\overline{u'u'}))$ are additional turbulent stresses on the mean flow components:

$$\frac{\partial U}{\partial t} + div(UU) = -\frac{1}{\rho} \frac{\partial P}{\partial y} + v div(grad(U)) + \frac{1}{\rho} \left[\frac{\partial(-\rho \overline{u'^2})}{\partial x} + \frac{\partial(-\rho \overline{u'v'})}{\partial y} + \frac{\partial(-\rho \overline{u'w'})}{\partial z} \right] \quad \dots (5)$$

Reynolds stress terms are non-zero due to the square. The numerical solution of the flow problem depends on the modeling of these extra terms such that the number of terms entering the model will affect its complexity and economy for flow prediction. The classical turbulence models such as k-ε model can express the turbulent main flow by one length scale and one time scale. The transport equations of turbulence kinetic energy, k , and its rate of dissipation, ε , can be presented as follows:

$$\frac{\partial(\rho k)}{\partial t} + div(\rho k \mathbf{U}) = div \left[\frac{\mu_t}{\sigma_k} grad k \right] + 2\mu_t S_{ij} \cdot S_{ij} - \rho \varepsilon \quad \dots (6a)$$

$$\frac{\partial(\rho \varepsilon)}{\partial t} + div(\rho \varepsilon \mathbf{U}) = div \left[\frac{\mu_t}{\sigma_\varepsilon} grad \varepsilon \right] + C_{1\varepsilon} \frac{\varepsilon}{k} 2\mu_t S_{ij} \cdot S_{ij} - C_{2\varepsilon} \rho \frac{\varepsilon^2}{k} \quad \dots (6b)$$

$$\mu_t = \rho C_\mu \frac{\varepsilon^2}{k} \quad \dots (7)$$

where:

- μ molecular viscosity (N. sec/m²)
- S_{ij} the mean deformation
- $C_{1\varepsilon}, C_{2\varepsilon}, C_\mu$ empirical constants having the values of 1.44, 1.92 and 0.09, respectively
- σ_k and σ_ε turbulent Prandtl numbers for k and ε having the values of 1.0 and 1.3, respectively.

Solving the partial differential equations of Navier-Stokes for engineering turbulent flow practices may be carried on by modelling rather than resolving (Wang and Chu, 2012). The computational fluid dynamic modelling software FLOW-3D developed and commercialized by Flow-Science Inc. includes five turbulence models. The standard k - ε model may be used when chaos flow and unstable motion of fluid flow occurs due to the generation of eddies of various sizes depending on **Re** especially when reaching high values (FLOW-3D Documentation, 2012). This model is "a more sophisticated – and more widely used – model consisting of two transport equations for the turbulent kinetic energy and its dissipation". The manual indicated that this model has been shown to provide reasonable approximations to many types of flow. Khazaee and Mohammadiun (2012) have declared this model as semi-empirical. Versteeg and Malalasekera (2007) also indicated that this model focuses on the mechanisms that affect k . As to the present case, the flow pattern over and pass the single step weir is simulated using the k - ε model since parts of the flow domain are turbulent.

GOVERNING EQUATIONS OF HEC-RAS

The Steady Flow model of HEC-RAS may be utilized to calculate water surface profiles for a single river reach, or a full network of channels (in natural channels or artificially constructed canals). It can be used to model subcritical, supercritical, and mixed flow regimes.



The flow is assumed to be steady (not time-dependent) and one-dimensional (the total energy head is the same for all points in a channel section and the velocity components in directions other than the flow direction are neglected). The equations for modelling the one-dimensional flow are derived from the conservation of mass and conservation of momentum. The water surface profile between two adjacent cross-sections, as illustrated in Figure (1), is computed by solving the energy equation:

$$Z_1 + y_1 + \alpha_1 \frac{V_1^2}{2g} = Z_2 + y_2 + \alpha_2 \frac{V_2^2}{2g} + h_e \quad \dots (8)$$

where:

- Z_1, Z_2 bed elevation at the cross sections (m)
- y_1, y_2 vertical depth of water at cross sections (m)
- V_1, V_2 average velocity of flow at cross sections (m/sec)
- α_1, α_2 velocity weighting coefficients at the cross sections
- h_e energy head loss (m).

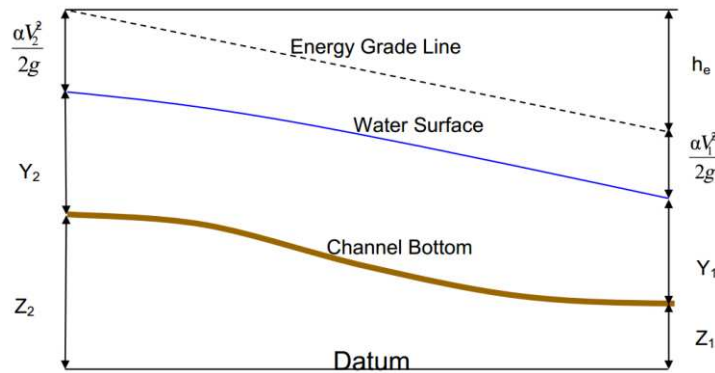


Figure (1): Terms of the energy equation (USACE, 2010).

A common cause of energy loss between two cross sections within a reach is the flow contraction or expansion due to changes in the channel cross section. HEC-RAS assumes that a flow contraction occurs when the velocity head increases in the downstream direction; and an expansion occurs when the velocity head decreases. The energy head loss includes friction losses and contraction/expansion losses and is given by:

$$h_e = \bar{S}_f L + C \left| \alpha_1 \frac{V_1^2}{2g} - \alpha_2 \frac{V_2^2}{2g} \right| \quad \dots (9)$$

in which C is the contraction or expansion coefficient, \bar{S}_f is the representative friction slope between two cross sections, computed using the average conveyance equation (10), and L is the discharge weighted reach length (m), computed by Equation (11):

$$\bar{S}_f = \left[\frac{Q_1 + Q_2}{A_1 R_1^{2/3} / n + A_2 R_2^{2/3} / n} \right]^2 \quad \dots (10)$$

where:

- n Manning's roughness coefficient (sec/m^{1/3})
- Q_1, Q_2 discharge at cross sections (m³/sec)
- A_1, A_2 flow area of cross sections (m²)
- R_1, R_2 hydraulic radius of cross sections (m).

$$L = \frac{L_{lob}\bar{Q}_{lob} + L_{ch}\bar{Q}_{ch} + L_{rob}\bar{Q}_{rob}}{\bar{Q}_{lob} + \bar{Q}_{ch} + \bar{Q}_{rob}} \quad \dots (11)$$

where L_{lob} , L_{ch} , L_{rob} are reach lengths of the left overbank, main channel and right overbank, respectively, and \bar{Q}_{lob} , \bar{Q}_{ch} , \bar{Q}_{rob} are the average flow rates between two sections in the main channel and the overbanks.

The energy equation is solved by the standard step method. In this method, the flow depth and velocity at one end of the channel reach are known. The reach length is known and the depth at the other reach end is calculated. For subcritical flow, the conditions at the downstream section are known. For a given discharge, Equation (8) can be expressed in terms of y_1 which will be the only unknown. The expression is implicit in y_1 , and is therefore solved using an iterative technique. Different values for y_1 are tried out until the equation is satisfied. For supercritical flow, the upstream conditions are known. Then, Equation (8) is solved iteratively to determine y_2 (Akan, 2006).

In the energy equation, the flow is assumed to be gradually varied, that is, the streamlines are parallel and the pressure distribution is hydrostatic at each channel section except at hydraulic structures. The channel is assumed to have a slope of 1:10 or less. This limit on the slope is based on the fact that the vertical pressure head, h , is computed as:

$$h = d \cos\theta \quad \dots (12)$$

$$d = y \cos\theta \quad \dots (13)$$

where d is the water depth measured perpendicular to the channel bottom and θ is the channel bottom slope expressed in degrees (Chow, 1959). For a slope of 1:10 (5.71 degrees) or less, $\cos(\theta)$ is 0.995. Thus, instead of using $d \cos(\theta)$, h is approximated as d and is used as y . This approximation results in a small error of (0.5 %) in estimating y . However, if HEC-RAS is used on steeper slopes, the computed water depths need to be corrected by dividing by $\cos(\theta)$ (USACE, 2010). In addition, the user must be aware that at very steep slopes air entrainment, and other possible factors that may not be taken into account, can be encountered.

Whenever the flow passes through critical, the energy equation is considered inapplicable since the transition from (sub to supercritical) or vice versa is a rapidly varying flow situation. These flow situations occur at specific locations such as (weir, drop, bridge, stream junction, changes in the channel slope). At these cases, HEC-RAS switches to the momentum equation or other empirical formula. The momentum equation is derived from Newton's second law of motion. Applying the law to a water body enclosed by two cross sections, as shown in Figure (2), the change in momentum with time is expressed as:

$$P_2 - P_1 + W_x - F_f = Q \rho \Delta V_x \quad \dots (14)$$

where P_1 , P_2 are the pressure force at sections 1 and 2, W_x is the force due to weight of water in the x direction, F_f is the force due to external friction losses from section 2 to 1, and ΔV_x is the change in velocity from section 2 to 1 in the x direction.

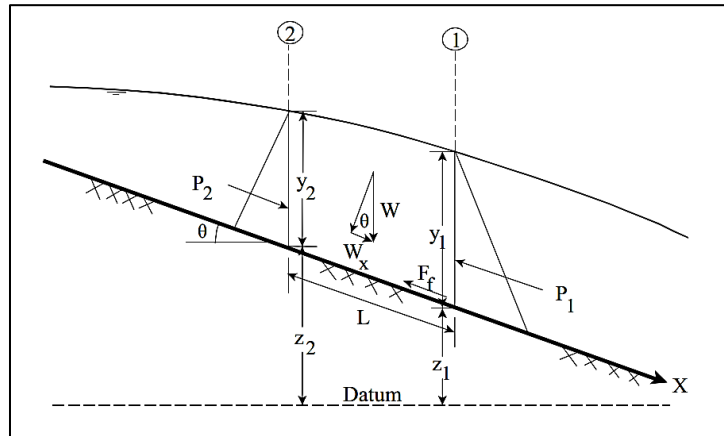


Figure (2): Terms of the momentum equation (USACE, 2010).

Substituting the forces and assuming Q varies from section 2 to 1, Equation (14) can be rewritten as:

$$\frac{Q_2^2 \beta_2}{g A_2} + A_2 \bar{Y}_2 + \left(\frac{A_1 + A_2}{2}\right) L S_0 - \left(\frac{A_1 + A_2}{2}\right) L \bar{S}_f = \frac{Q_1^2 \beta_1}{g A_1} + A_1 \bar{Y}_1 \quad \dots (15)$$

where β_1, β_2 are Boussinesq momentum coefficients at the cross sections, \bar{Y}_1, \bar{Y}_2 are flow depth measured from surface to the centroid of the area of cross section 1 and 2, and S_0 is the slope of the channel, based on the mean bed elevations.

MODEL SIMULATIONS

The geometry of the numerical model was constructed by the geometric tools of the software. The computational domain was set to 4 m length, 0.3 m width and 0.4 m height. The single-step weir was incorporated at 2.61 m from the upstream end of the channel, as shown in Figure (3) and (4).

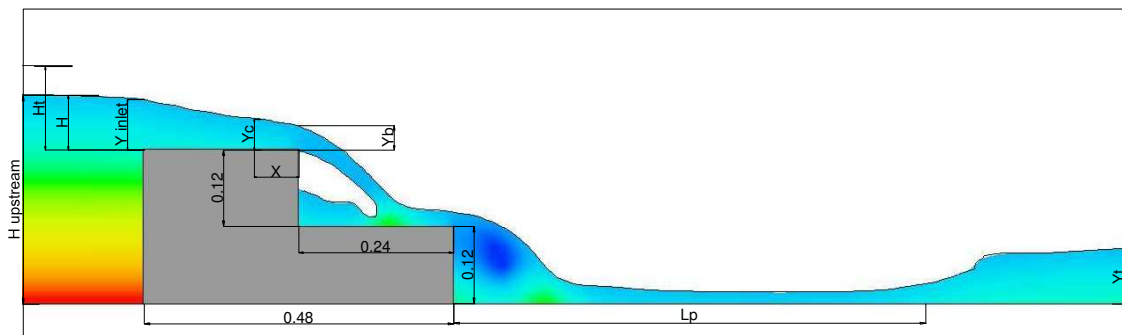


Figure 3: Definition of physical geometry and flow parameters, FLOW-3D.

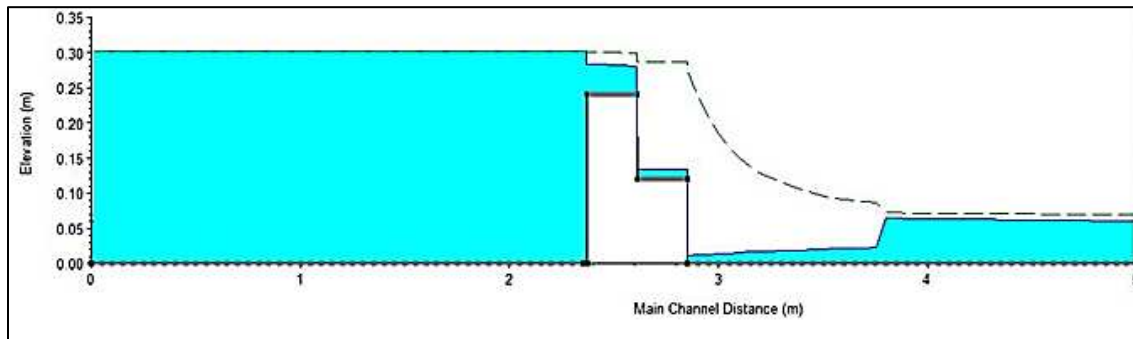


Figure 4: Definition of physical geometry and flow pattern, HEC-RAS.

According to earlier studies, the smaller the mesh size the greater is the accuracy and the more is the computational time. In the $k-\varepsilon$ model, the domain was discretized in finite volume of cubes starting from 2 cm then it was decreased to 1 cm to reduce the error in the flow profile but the computational time increased two times or more depending on the value of the flow rate. The boundary conditions were fixed as symmetry at the top and the channel sides while the bottom as a wall, the downstream as pressure corresponding to the experimental sequent depths of the jump. The upstream conditions were set to the inflow rate of the experimental data. The same model set-up was used in all models such that incompressible flow, viscous flow, free surface or sharp interface, gravitational acceleration in the vertical direction and nonslip wall shear boundary were selected.

FLOW-3D is designed to fit time dependent 3-D free flow. Its pressure-velocity coupling algorithms arise from two special numerical techniques based on semi-implicit formulation of iteration: Successive over Relaxation (SOR) and Generalized Minimum Residual (GMRES) (FLOW-3D Documentation, 2012). The two solvers show fairly similar computational results. The difference between them is the iteration steps, SOR solver is similar to Jacobi and GMRES solves fully coupled system of equations so it needs little more time for computations.

On the other hand, the modelling process in the Steady Flow model of HEC-RAS is relatively simple for the present hydraulic problem. First, the channel schematic represented by a straight line was drawn from upstream to downstream. Next, it was discretized into segments with their lengths ranging from 5 cm in the uniform-flow region to 1 cm in the varied-flow region. The geometric data were entered along the channel including the cross section coordinates, reach length, Manning's roughness coefficient for friction losses, and the contraction and expansion coefficients for transition losses.

The Steady Flow Component of HEC-RAS requires specifying number of the flow profiles to be computed, flow rates, and the boundary conditions. The observed flow rates, overflow depths, and tailwater depths were used as boundary conditions in the model. After entering the data, the mixed (subcritical and supercritical) flow regime was used for the computations. In HEC-RAS, the momentum equation is used within the mixed flow regime. The flow profile over the single-step weir is characterized by a change from subcritical to supercritical flow due to the drop, and from supercritical to subcritical flow due to the hydraulic jump. Therefore, the mixed flow regime was adopted.

EXPERIMENTAL MODELLING

The experimental work was carried out using a horizontal rectangular channel having a working length of 5 m, a width of 0.3m and depth of 0.45m. The tested weir is 48 cm long and 24 cm high, the weir includes a single step at the downstream, the step length is 24 cm and the height is 12 cm. The weir model is made from a transparent plastic plate of 6 mm thickness. The inflow rate was measured by an electro-magnetic flow meter and the water depths were measured using manual

point gauges. The tail water depth downstream of the hydraulic jump was controlled using a tilting gate located at the downstream end of the channel.

Fourteen different inflow rates were applied to the weir. Eleven runs were observed to be of type *true broad-crested weir flow*, with the ratio of the energy head to the length of the weir crest between $(0.1 < h/L_w \leq 0.35)$ (Subramanya, 1986) and three runs were of type *narrow-crested weir flow* with h/L_w less than 0.55.

RESULTS AND DISCUSSION

For the purpose of comparison, the flow domain was separated into four regions based on the type of flow and its turbulence. The first part is the flow region upstream and over the weir crest before the nappe fall occurs. The water surface profiles upstream the weir are shown in Figure (5a). For the purpose of clarity, profiles of only eight flow rates are displayed. From the plots, it can be visually noticed that the measured and computed profiles are in good agreement with some deviation in the HEC-RAS profiles just before the weir. This is believed to be due to the significant curvature of the streamlines where the hydrostatic pressure distribution is assumed in the energy equation for the gradually varied flow.

The flow profiles over the weir crest are displayed in Figure (5b), which shows that HEC-RAS estimated lower depths than the measured depths before the control section on the weir crest and higher depths after that, which means higher brink depths, y_{br} , especially at higher flow rates. However, the critical depth, y_c , was predicted with satisfactory accuracy.

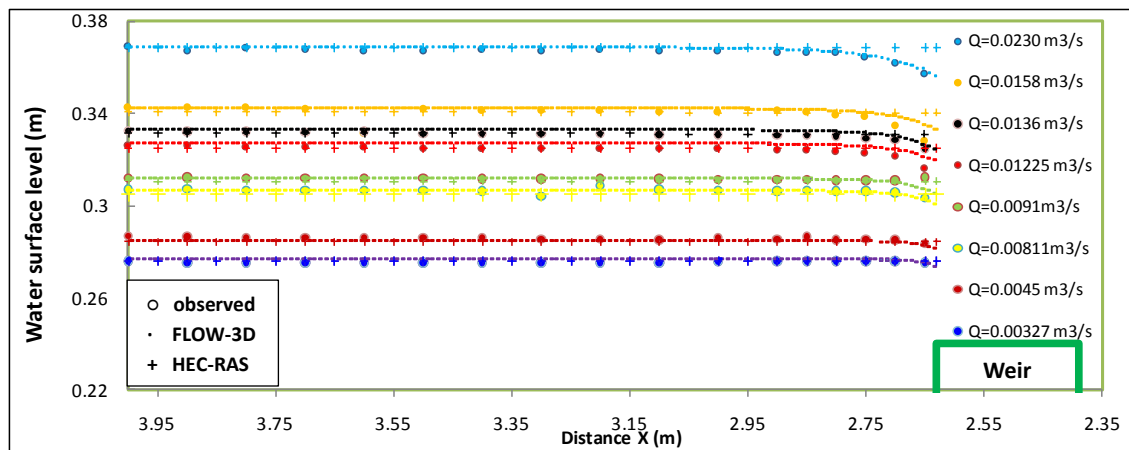


Figure 5a: Comparison of the flow profiles upstream the weir

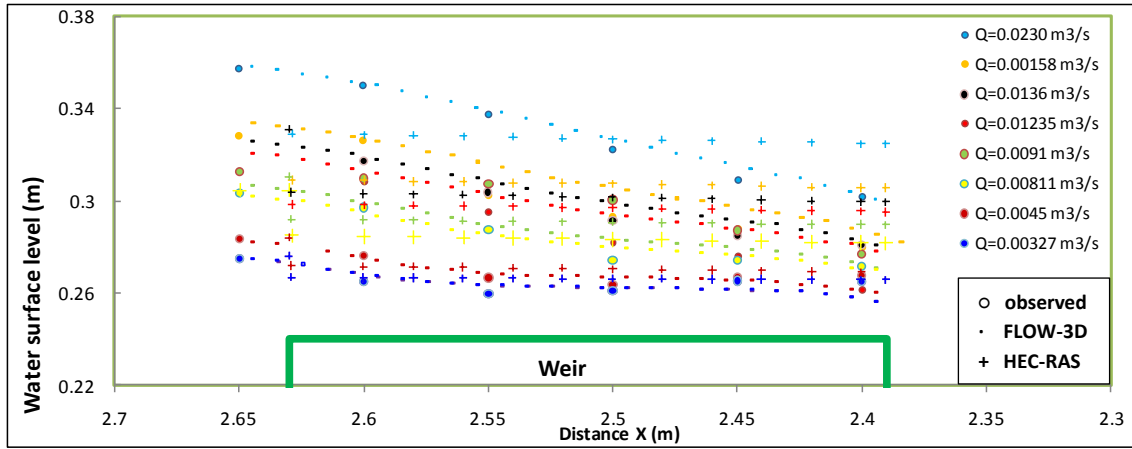


Figure 5b: Comparison of the flow profiles over the weir crest

The critical depths on the weir crest estimated by the two models are compared with the theoretical values in Figure (6). It is obvious that the estimated critical depths are highly correlated to the flow rates and are nearly similar to the theoretical values with little over-estimation from FLOW-3D and little under-estimation from HEC-RAS. This may be related to the type of flow profile generated over the crest depending to the value of (h/L_w) .

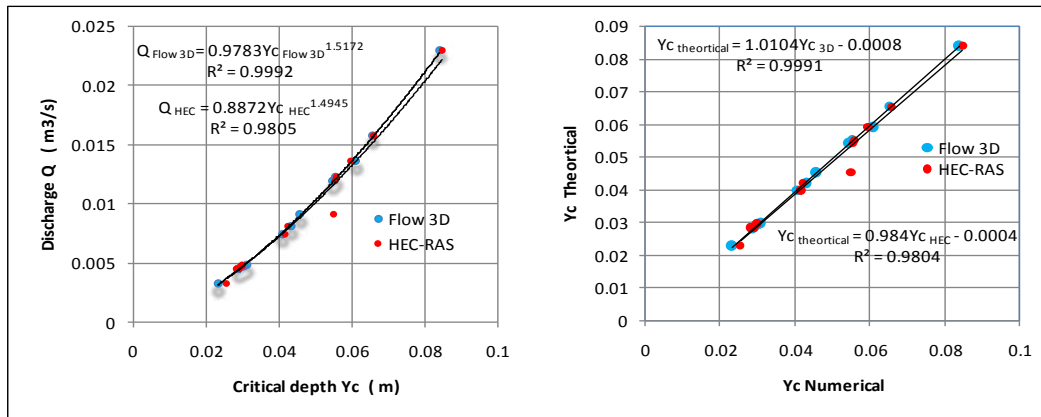


Figure 6: Comparison of the critical depth predicted by HEC-RAS and FLOW-3D.

Furthermore, the relation between y_c and y_b predicted by each numerical model has been studied in accordance with the earlier basic findings of Chow (1959), as presented in Figure (7). In fact, due to the significant curvature of flow near the brink, y_b is less than y_c for a given flow rate. Chow has fixed the (y_d/y_b) ratio to 1.5, but HEC-RAS produced an average value of 1.0193 versus 1.5687 in FLOW-3D. It can be observed that FLOW-3D could better predict this ratio than HEC-RAS, which predicted higher y_b values and thus produced lower ratios.

In addition, descriptive statistics was carried on to find out the inaccuracy in the numerical simulations of the flow profile. The part of flow upstream the weir is characterized by the Froude Number in the range $0.024 < Fr < 0.11$ and Reynolds Number $1.5 \times 10^4 < Re < 9 \times 10^4$. Table (1) shows the inaccuracy in the predicted results for this flow region. The percent mean error is -0.02% in HEC-RAS and -0.51% in FLOW-3D, while the average absolute error is 0.52% and 0.59%, respectively. These results show good agreement with observed profiles for the given ranges of **Fr** and **Re**.

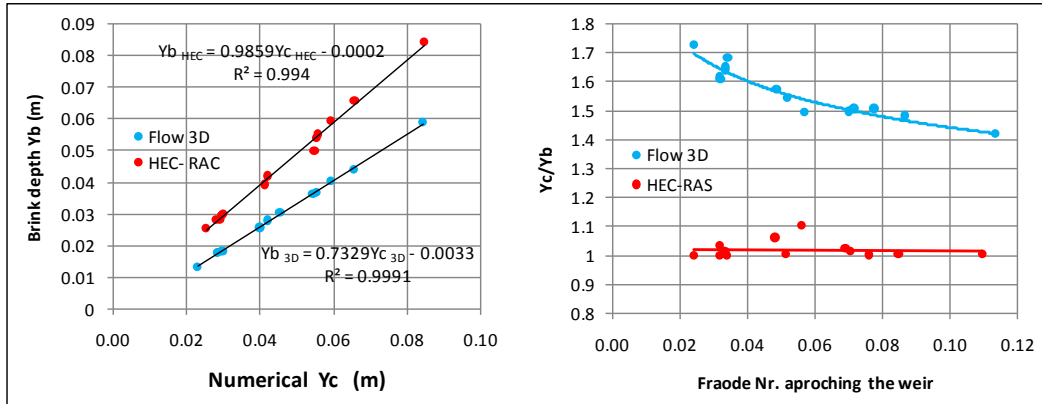


Figure 7: Comparison of the relation between y_c and y_b predicted by HEC-RAS and FLOW-3D.

Table (1): Descriptive statistics for the flow region upstream the weir.

	N	Range	Minimum	Maximum	Mean		Std. Deviation	Variance
	Statistic	Statistic	Statistic	Statistic	Statistic	Std. Error	Statistic	Statistic
HEC-RAS Relative error %	196	3.8223	-2.6546	1.1677	-.021508	.0542888	.7600427	.578
Flow 3D Relative error %	196	3.9543	-3.4155	.5388	-.513383	.0589488	.8252836	.681
Valid N (listwise)	196							

The flow over the weir crest is qualified by $0.60 < Fr < 1.60$ and $3.6 \times 10^4 < Re < 2 \times 10^5$. The comparison of the observed and the computed free surface profiles shows some differences between the two numerical models, as discussed formerly. HEC-RAS gives a percent mean error of -1.53% and an average absolute error of 2.48%. In the other hand, FLOW-3D gives the mean relative error of -0.94% and average absolute error is 1.57 %, as shown in Table (2). Thus, FLOW-3D illustrates its advantage in simulating the gradually varied flow profile in this region where the flow state changes from subcritical to supercritical.

Table (2): Descriptive statistics for the flow profile on the weir crest.

	N	Range	Minimum	Maximum	Mean		Std. Deviation	Variance
	Statistic	Statistic	Statistic	Statistic	Statistic	Std. Error	Statistic	Statistic
HEC-RAS Relative error % on weir	113	19.2990	-13.2133	6.0857	-1.527196	.2857663	3.0377375	9.228
Flow 3D Relative error % on weir	113	12.1716	-6.5473	5.6244	-.936032	.1783826	1.8962331	3.596
Valid N (listwise)	113							

The second part of the flow domain is the region downstream the crest of the weir. It includes the nape flow and the hydraulic jump. The observed and simulated water surface profiles for the nape falling from the weir crest are displayed in Figure (8a). It can be seen that HEC-RAS could not well simulate the nape flow; the computed profiles are nearly horizontal on the step. The graphs reveal that HEC-RAS cannot produce curved profiles past vertical faces while FLOW-3D presents better simulation in this part of flow. This is attributed to the different governing equations and the different solution approaches followed by the two models.

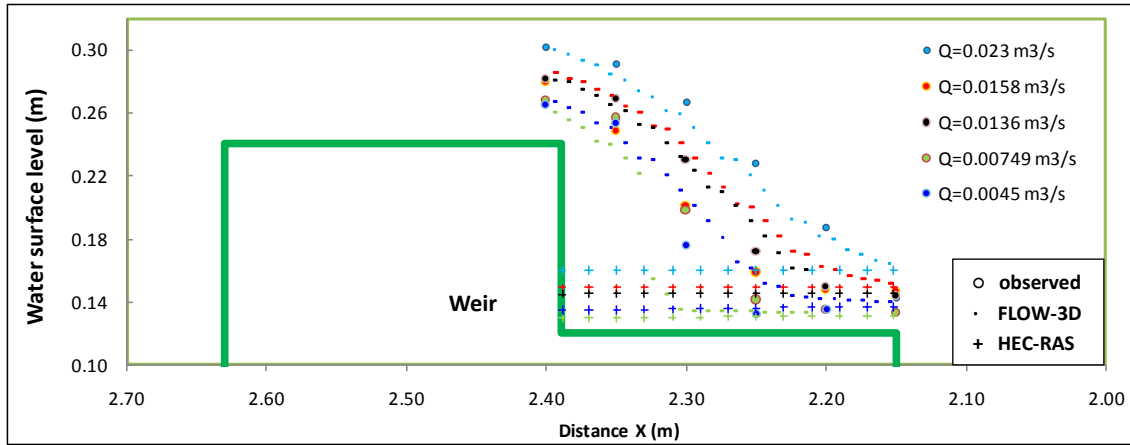


Figure 8a: Comparison of the flow profiles downstream the weir crest

The position and characteristics of the hydraulic jump occurring downstream the weir depends on the flow rate and the tail water depth, y_2 . The hydraulic jumps observed in the laboratory channel involved different types of free jumps and some submerged jumps. The chaos behavior of the falling flow was easily observed in the channel. This flow region was characterized by $1.05 < Fr < 5.4$ and $6 \times 10^4 < Re < 2.5 \times 10^5$, which can be described as a fast-moving stream with turbulent eddies. The scale of chaos in the turbulent flow affects the experimental data as well as the simulated flow. Measuring the flow depths accurately at these fluctuating regions was not possible with the available apparatus used in the present laboratory work, especially at the toe of the weir, as can be seen in Figure (8b).

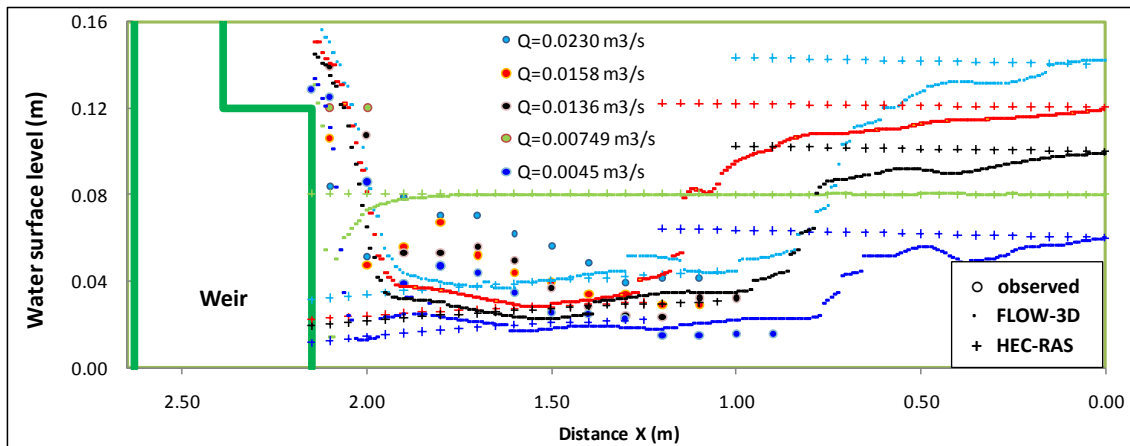


Figure 8b: Comparison of the flow profiles downstream the weir

Concerning the flow part downstream to the jump, FLOW-3D did not show acceptable profile. The inaccuracy in the predicted profile was 13.95% versus -8.97% in HEC-RAS, which simulated this profile as a horizontal line and did not show the shape of the jump. This flow region exhibits high turbulence with Re reaching up to 2.5×10^5 and Fr up to 5.4 revealing the occurrence of hydraulic jumps that are mainly of three types (undular, weak and oscillating) characterized by a marked roller and wavy free surface. The disturbances grow and propagate in the whole region of flow when Re

reaches to high values and water particles follow irregular paths that may not be continuous (Chanson, 2004). This large diversion from the experimental results at the downstream region may also be attributed to the air interference which is not accounted for in the numerical analysis. The location of the hydraulic jump at the downstream end of the channel was also studied. The dimensionless parameter (L/y_t) was used for this purpose, where L is the distance from the weir to the jump. This parameter was used to compare the jump position predicted by the software, as presented in Figure (9). The comparison shows that there is good agreement between the observed and computed results. The output data collected from FLOW-3D are better correlated than those from HEC-RAS.

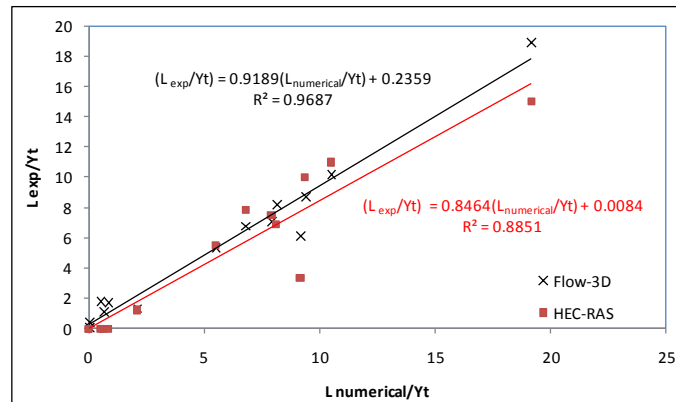


Figure 9: Comparison of the observed and predicted locations of the hydraulic jump.

CONCLUSION

The free flow over the single-step weir is studied experimentally in an open channel and simulated numerically. Two modelling systems were compared throughout the flow domain. The analysis was carried out in parts depending on the type of flow in each region. From the analysis of the experimental data and the simulation outputs, the following conclusions may be forwarded:

- In the flow region upstream the weir where **Fr** and **Re** have low values, the water surface profiles computed by HEC-RAS and FLOW-3D were in good agreement with the observed ones with average absolute error of 0.52% and 0.59%, respectively.
- The gradually varied flow over the weir crest was well simulated by FLOW-3D with average absolute errors of 1.57% against 2.48% in HEC-RAS. The profile computed by HEC-RAS had discontinuity at the weir corners.
- The critical depth over the weir crest was well predicted by the two numerical models.
- HEC-RAS predicted higher brink depths, especially at higher flow rates.
- The relation between the critical depth and the brink depth was well established by the two models, especially FLOW-3D.
- The (y_d/y_b) ratio was 1.0193 in HEC-RAS versus 1.5687 in FLOW-3D, compared to value of 1.5 defined by Chow.
- HEC-RAS has limited ability to produce curved profiles past vertical faces, thus, it did not present good simulation for the nape flow falling from the weir crest and step while FLOW-3D did.

- The turbulences in the hydraulic jump regions were not well simulated by the adapted FLOW-3D ($k-\epsilon$) turbulent model and the Steady Flow model of HEC-RAS. However, accurate measurement of the flow depths at these fluctuating regions was also not possible.
- The location of the hydraulic jump at the downstream end of the channel was predicted with adequate accuracy by both models.
- FLOW-3D is more capable of simulating the rapidly varied flow.
- HEC-RAS is economically more attractive to predict water surface profile for long channels with less events of rapidly varied flow. Such problems if modeled using FLOW-3D, they will take relatively long time.

REFERENCES

1. Akan, A. O. (2006), *Open Channel Hydraulics*, First edition, Elsevier.
2. Akbar, Z.A.; Habib, M.J.S.; Hassan, L.: Simulation of Hydraulic Jump through Channels Junction Using the FLOW-3D and Fluent Models, *Research Journal of Recent Sciences*, 4(1), 129-134 (2015).
3. Babaali, H.; Shamsai, A.; Vosoughifar, H.: Computational Modeling of the Hydraulic Jump in the Stilling Basin with Convergence Walls Using CFD Codes, *Arabian Journal for Science and Engineering*, 4(2), 381–395 (2015).
4. Chanson, H.: *The Hydraulics of Open Channel Flow: An Introduction*, Second edition, Elsevier (2004).
5. Chow, V.T.: *Open-Channel Hydraulics*, McGraw-Hill (1959).
6. Cook, A.C.: Comparison of One-Dimensional HEC-RAS with Two-Dimensional FESWMS Model in Flood Inundation Mapping, MSc thesis, Purdue University, USA (2008).
7. Crookston, B.M.; Paxson, G.S.; Savage, B.M.: Hydraulic Performance of Labyrinth Weirs for High Headwater Ratios, The 4th IAHR International Symposium on Hydraulic Structures, Porto, Portugal, 1-8 (2012).
8. FLOW-3D Documentation, Release 10.1.0, Flow Science, Inc. (2012).
9. Graebel, W.P.: *Advanced Fluid Mechanics*, Elsevier (2007).
10. Gonzalez, N.S.: Two-Dimensional Modeling of the Red River Floodway, MSc thesis, University of Manitoba, Canada (1999).
11. Hoseini, S.H.: 3D Simulation of Flow over a Triangular Broad-Crested Weir, *Journal of River Engineering*, 2(2), 1-7 (2014).
12. Khazaei, I.; Mohammadiun, M.: Effect of flow field on open channel flow properties using numerical investigation and experimental comparison, *International Journal of Energy and Environment*, 3(4), 617-628 (2012).
13. Mohammed, J.R.; Qasim, J.M.: Comparison of One-Dimensional HEC-RAS with Two-Dimensional ADH for Flow over Trapezoidal Profile Weirs, *Caspian Journal of Applied Sciences Research*, 1(6), 1-12 (2012).
14. Rady, R.M.: 2D-3D Modeling of Flow over Sharp-Crested Weirs, *Journal of Applied Sciences Research*, 7(12), 2495-2505 (2011).
15. Siddique-E-Akbor, A.H.M.; Hossain, F.; Lee, H.; Shum, C.K.: Inter-comparison study of water level estimates derived from hydrodynamic–hydrologic model and satellite altimetry for a complex deltaic environment, *Remote Sensing of Environment*, Vol. 115, 1522–1531 (2011).
16. Subramanya, K.: *Flow in Open Channels*, McGraw-Hill (1986).
17. Toombes, L.; Chanson, H.: Numerical Limitations of Hydraulic Models, The 34th International Association for Hydraulic Research World Congress, Brisbane, Australia, 2322-2329 (2011).

18. U.S. Army Corps of Engineers: HEC-RAS River Analysis System, Hydraulic Reference Manual, Version 4.1, Hydrologic Engineering Center, Davis, California (2010).
19. Versteeg, H.K.; Malalasekera, W.: An Introduction to Computational Fluid Dynamics, Second edition, Pearson Education Limited England (2007).
20. Wang, T.; Chu, V.H.: Manning Friction in Steep Open-channel Flow, The 7th International Conference on Computational Fluid Dynamics, Big Island, Hawaii (2012).

پوخته

لهم توپژینه وهیهدا دوو بهرنامه FLOW-3D ($k-\epsilon$ model) و HEC-RAS (Steady-Flow model) بهکارهینراون بؤ لاساییکردنی رۆیشتنی ئاو له سهر بهر بهستی لوتکه پانی تاکه پایهدا. نهجمهگانی لاساییکردنی ژمارهیی بهراوردکران له گهل نهجمهگانی نیشی تافیگه که پیکهاتبوون له چهنهین دوخی هایدرولیکی جیاواز. ههر دوو بهرنامه توانییان وهسفی رۆالهتی رۆیشتنی ئاو له پیش بهر بهستی بکهن به ریژهی ههلهی 0.52% و 0.59%. ههر وهها بینراوه که FLOW-3D دهتوانیت وهسفی باشتر بکات بؤ رۆیشتنی گوراوی وردهوردهی ئاو له سهر بهر بهستی به ریژهی ههلهی 1.57% بهرانبهر 2.48% له HEC-RAS. دیسان بینراوه که HEC-RAS بهرزیکی زیاتر دردههینیت بؤ ناستی ئاو له سهر لیوهی بهر بهستی بهتایبهت له دوخهگانی ریژهی زووری رۆیشتن. بهرنامهگان ههر وهها پیشبینی باشیان کرد بؤ ناستی ناوی کریتیکهل وپهیهوندیهکهی له گهل ناستی سهر لیوه، FLOW-3D ریژهی (y_c/y_b) به 1.5687 خهملاند بهرانبهر 1.0193 له HEC-RAS. سهبارت به شیوهی کهوتنه خوارهوهی ئاو له لوتکه وپایهیی بهر بهستدا، نهوا HEC-RAS نهیتوانی به جوانی نهام پارچهیه وهسفی بکات به هوی شیانهگانی سنووردار له پشاندانی پرۆفایلی چهماوهی له دواي روهی ستوون، به بهراورد له گهل FLOW-3D. له لایهکی ترهوه، بهرنامهگان ههر دووگیان به وردی رۆیشتنی سوپهر کریتیکهل له پیش بازی ناوی لاسایی یان نهکرد بهلام باش شوینی باز دیاریان کرد.

الخلاصة

في هذه الدراسة تم محاكاة الجريان الحر فوق الهدار عريض الحافة مفرد الدرجة باستخدام FLOW-3D ($k-\epsilon$ model) و HEC-RAS (steady-flow). تم التحقق من صحة نتائج هذه البرامج بمقارنتها بالبيانات المختبرية التي تضمنت أوضاع جريان مختلفة. أظهرت البرامج قابليتها للتنبؤ بشكل الجريان قبل الهدار بنسبة خطأ 0.52% و 0.59%. بينما أظهر FLOW-3D قابلية أفضل لحساب الجريان المتغير التدريجي فوق قمة الهدار بنسبة خطأ 1.57% مقابل 2.48% في HEC-RAS. بالإضافة إلى ذلك، فإن HEC-RAS أعطى قيم أعلى لعمق الماء على الحافة مقارنة ب FLOW-3D خاصة في حالة التصاريح العالية. كما حسبت البرامج عمق الماء الحرج وعلاقته بعمق الحافة بدقة مرضية. حَمَن FLOW-3D نسبة (y_c/y_b) ب 1.5687 مقابل 1.0193 في HEC-RAS. بالنسبة للجريان الساقط من قمة ودرجة الهدار، فإن HEC-RAS لم يقدم وصفاً جيداً لشكل الجريان وذلك لقابليته المحدودة على أظهار الشكل المنحني للجريان مقارنة ب FLOW-3D. من ناحية أخرى فإن كلاً منهما لم يصف الجريان فوق الحرج قبل القفزة الهيدروليكية بكفاءة ولكن قدر موقع القفزة بشكل جيد.